Deconvolution of the X-ray "Illite" 10 Å complex : a case study of Helvetic sediments from eastern Switzerland

Autor(en): **Wang, Heijing / Stern, Willem B. / Frey, Martin**

Objekttyp: **Article**

Zeitschrift: **Schweizerische mineralogische und petrographische Mitteilungen = Bulletin suisse de minéralogie et pétrographie**

Band (Jahr): **75 (1995)**

Heft 2

PDF erstellt am: **25.04.2024**

Persistenter Link: https://doi.org/10.5169/seals-57150

SCHWEIZ. MINERAL. PETROGR. MITT. 75, 187–199, 1995

Deconvolution of the X-ray "Illite" 10 Å complex: a case study of Helvetic sediments from eastern Switzerland

by *Heijing Wang*[1,2], *Willem B. Stern*[2] and *Martin Frey*[2]

Abstract

The clay mineral X-ray diffraction complex around 10 Å of 381 samples (air-dried, glycolated) of Helvetic sediments from eastern Switzerland was studied with a Siemens D-500 and a Philips PW-1361 diffractometer using Cu-Kα radiation. In contrast to the first basal reflection of muscovite single crystals, all 10 Å peaks examined were asymmetric showing a tailing on the long-wavelength side. Assuming the presence of at least two not always resolved reflections of illite-muscovite and a smectitic phase displaying different d-values, half-widths and heights, a mathematical deconvolution of the 10 Å complex was executed by means of Pearson functions in order to determine the peak parameters. The second, smectitic phase is either documented by the FWHM-difference (FWHM = Full width at half peak maximum) of the air-dried vs glycolated complex, or by the FWHM-difference of the air-dried complex vs deconvoluted illite. On the average, it begins to disappear in the mid-anchimetamorphic realm.

The FWHM of deconvoluted illite and the smectitic phase generally decrease in the study area from Appenzell in the north to Chur in the south with increasing diagenetic/metamorphic grade, as do the d-values of the smectitic phase. By correlating the overall FWHM of the unresolved complex (Kübler-/Scherrer-Index) with deconvoluted data, the metamorphic limits were determined for (air-dried) deconvoluted illite and smectitic phase. The epizonal/anchimetamorphic limits of $\Delta°2\Theta = 0.25$ for the unresolved, air-dried complex remain the same for the tested Philips PW-1361 diffractometer and for the Siemens D-500, as do the anchimetamorphic/diagenetic boundaries with $\Delta°2\Theta = 0.42$. In diagenetic and anchimetamorphic air-dried specimens the variation of the 10 Å complex is predominantly due to the d-, FWHM-, area-variations of this second, smectitic phase rather than to variations of illite sensu stricto.

Keywords: incipient metamorphism, illite crystallinity, X-ray diffraction, Helvetic nappes.

Introduction

Shape and intensity of X-ray reflections are influenced by several factors, like instrument optics, domain/particle size, strain effects, interference with other reflections, crystallographic parameters, mass fraction of the measured phase, and orientation effects. Since the early days of powder diffractometry, efforts have been made to deconvolute X-ray reflections mathematically (LAUE, 1926), but only recently deconvolution programs have become generally available on PC-based instrumental systems.

Fitting as a method of peak modelling, and deconvolution for the evaluation of overlapping reflections (line interference) are not only essential for the quantification of d-value, FWHM and peak area, but also for domain size and strain studies. An overview of the topic, and of earlier work can be found in KLUG and ALEXANDER (1974), and DELHEZ et al. (1982) giving details on different approaches, such as the Warren-Averbach and the Rietveld methods. Recent computations were published by LANSON and BESSON (1992), VELDE and LANSON (1993), STERN et al. (1991), WANG (1994).

The importance of the FWHM of the clay mineral complex around 10 Å as an indicator of incipient metamorphism was stressed by KÜBLER in 1968 already. Since then it has been used

[1] Present address: Dept. of Geology, Peking University, Beijing 100871, PR China.
[2] Mineralogisch-Petrographisches Institut, Bernoullistrasse 30, CH-4056 Basel, Switzerland.

worldwide as a fast and simple description of incipient metamorphism of clay containing sediments.

The purpose of the present study is to examine whether deconvolution techniques with their ability to quantify several relevant variables such as FWHM, d-value, peak area, curve exponent (Pearson function) of both, illite and smectitic phase (see below), are able to refine the mapping of incipient metamorphism. This is especially true in the diagenetic realm, where half-width determinations of the unresolved complex become specifically difficult, or even impossible when e.g. paragonite is present as an additional phase.

Methodological aspects

An uncertainty of nomenclature exists with respect to the second phase present besides illite in the 10 Å complex of diagenetic and anchimetamorphic specimens. This phase is expandable under glycol, but never reaches 17 Å, which would be a prerequisite to call it smectite. Since it forms in diagenetic samples, however, a distinct additional reflection of its own, clearly separated from chlorite (001) on one side, and from the illite first basal reflection on the other which it never replaces (Fig. 1), it is labelled here tentatively as "smectitic phase". Alternatively, one could call it in a general sense a "mixed layer", consisting of two or more mineral phases, namely illite, smectite, ..., chlorite. The term I/S mixed-layer should be applied only when certainty exists about the exclusive presence and identity of the two minerals illite and smectite.

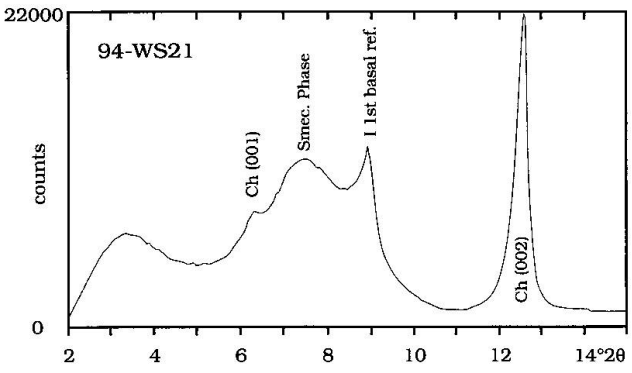

Fig. 1 Low-angle diffractogram of a typical diagenetic < 2 micron fraction (air-dried). Besides chlorite and illite-muscovite an additional, expandable phase occurs, whose d-value, half-width, shape and size is connected with metamorphic grade, and possibly bulk chemistry. Its strongly changing peak position (d-value) obscures the first basal reflection of illite such that a half-width determination of the latter is impossible without fitting/deconvoluting the entire complex into its respective fractions (chlorite, illite-muscovite, smectitic phase).

There exist at least two problems when the 10 Å complex of clay mineral phases has to be unraveled. The first is counting statistics, the second a tailing phenomenon which interferes with the peak overlap of illite and the smectitic phase. As studies of glycolated < 2 micron fractions of epizonal specimens prove, a more or less prominent tailing persists when no smectitic phase is expected. This kind of tailing is, however, neither present in well crystallized, mechanically undisturbed – i.e. not crushed or ground – sheet silicates, nor e.g. in clay mineral standards which were prepared without a strong mechanical grinding impact. This implies that the observed peak asymmetry is not defined by any instrumental factors of the diffractometer involved (STERN et al., 1993, 1995) as show in figures 2 a, b.

The low crystallinity of clay minerals induces not only a large FWHM and broad base lines, but also small peak intensities, and therefore poor counting statistics, which are in turn a handicap for any kind of mathematical deconvolution or peak fitting. Sometimes curve smoothing is recommended (LANSON and CHAMPION, 1991), but smoothing clearly tends to falsify the primary data, e.g. when d-values have to be evaluated. In the present study, care was taken to improve counting statistics experimentally by measuring the low angular range between 2 and 15 °2Θ with a very slow goniometer speed, see table 1a for instrumental settings.

Appropriate counting statistics provided, the reliability of a mathematical fitting/deconvolution process depends on the actual shape of the reflection, the type of function used (Gauss, Lorentz, Voigt, Pearson) on one hand (Fig. 2c), and on the number of phases taken into consideration for deconvolution on the other. It is obvious, that with rising number of curves involved, the reliability – correspondence of fitted and measured curves – is improved artificially. As a general rule, however, the number of curves should equal the number of mineral phases/reflections involved. For air-dried specimens, the number of phases was assumed to be three, namely illite, a smectitic phase and chlorite. In a few cases four phases were used including paragonite, which was identified by its (005) reflection. For glycolated diagenetic specimens four reflections were assumed, namely illite, chlorite and two reflections for the smectitic phase. The calculated reliabilities in the present study were all better than 10%, with three quarters being below 6% (air-dried), whereas 95% of the glycolated ones were below 7%.

A further essential boundary condition defining the quality of deconvolution, and of half-width determination in general, is background modelling. Since the background at low angles is not necessarily horizontal or flat (though an automatic entrance slit was used, Tab. 1a), its slope and curvature has to be taken into account when peak height and full width at half peak maximum are determined. All deconvolutions were executed under comparable boundary conditions (background subtraction, number of reflections, curve type) in order to keep systematic errors minimal.

Material studied: 381 samples were measured. Lithologies included 40% shales and slates, 30% sandstones, 20% marls, and 10% limestones and marbles. The location of the samples is given on figure 3. Note the uneven sample density (few samples W of Sargans and in the most southern part of the study area).

Sample preparation: samples were cleaned with a steel brush, crushed into small pieces with a hammer, and approximately 70 g of sample were ground in a tungsten-carbide disc-mill for 30 seconds. Carbonate was removed by treating with 5% acetic acid and by washing with deionized water. The < 2 micron fraction was prepared using differential settling tubes and millipore filters with 0.1 μm pore size. The clay fraction was then Ca-saturated with 2N $CaCl_2$. Oriented slides were prepared by pipetting suspensions onto glass slides (5 mg/cm²) and allowing to air-dry. Glycolated mounts (for 228 samples) were prepared in a glycol vapor bath at 60 °C overnight. 48 heat-treated samples were prepared in an oven at 500 °C for 1 h.

X-ray diffraction: all measurements were performed with a Siemens D-500 diffractometer, optimized for counting statistics, see table 1a. The angular increment ("step size") was 0.05 °2Θ for measuring angles below 14 °2Θ, and 0.02 °2Θ above, in order to obtain both, good counting statistics and acceptable resolution.

All specimens were also measured with a Philips PW-1361 diffractometer for control of data-consistency, because many published crystallinity data were obtained with this kind of diffractometer, table 1b.

Geological setting

The study area is located in the NE of Switzerland and extends from Appenzell in the north to Chur in the south (45 km) and from Lake Walen in the west to the Rhine River in the east (30 km), see figure 4. Tectonically the study area belongs to the Helvetic zone along the northern margin of the Alps. To the north the nappes of the Helvetic zone override the Tertiary clastics of the adjoining Molasse basin, a foredeep which formed during the later stage of the Alpine collision. To the south and east, the Helvetic nappes are overlain by the Penninic nappe system. The Mesozoic sediments making up the largest part of the Helvetic zone comprise essentially a carbonate shelf sequence of the northern European margin. In the course of the Alpine collision the Penninic nappes were thrust onto the Helvetic zone. During this process, the rocks of the Helvetic zone were buried, deformed and metamorphosed up to lower greenschist facies conditions.

The Helvetic zone of the investigated area is subdivided by the Glarus thrust, which has a displacement of up to 40 km, into the Helvetic nappes (above) and the Infrahelvetic complex (below). The Helvetic nappes represent classic detachment tectonics, whereas the Infrahelvetic complex is a thick skinned fold-and-thrust belt, cored by the Aar massif basement uplift. The stratigraphic sequence of the Helvetic zone includes Permian conglomerates, Triassic dolomites, various thick limestones of Jurassic and Cretaceous age and Tertiary sandstones that are interbedded with various shaly and marly horizons. For more detailed information on the geologic evolution of the Helvetic zone, the reader is referred to TRÜMPY (1980).

Very low grade metamorphism of the Helvetic zone of eastern Switzerland has been studied by many authors, using mainly the illite crystallinity technique and index minerals, supplemented by a few vitrinite reflectance and fluid inclusion data. FREY (1970) noted a general increase of illite crystallinity from the lower anchizone south of Lake Walen to the epizone in the parautochthonous cover of the Aar massif. FREY (1988) found epizonal illite crystallinities in the Verrucano of the lower Helvetic nappes and mid-anchizonal values in the underlying flysch units of the Infrahelvetic complex. The discontinuous inverse metamorphic zonation was explained by post-metamorphic thrusting along the Glarus thrust. FREY et al. (1973) and FREY (1987a) mapped index minerals in glauconite-bearing limestones. A stilpnomelane-in reaction-isograd was located in the mid-anchizone and a biotit-in reaction-isograd at the beginning of the epizone. FREY (1987b) located the reaction-isograd kaolinite + quartz = pyrophyllite + H_2O, running in a WSW–ENE direction close to the end of Lake Walen, and estimated metamorphic conditions at the reaction-isograd from vitrinite reflectance and fluid inclusions data to be 1.3 to 2.1 kbar and

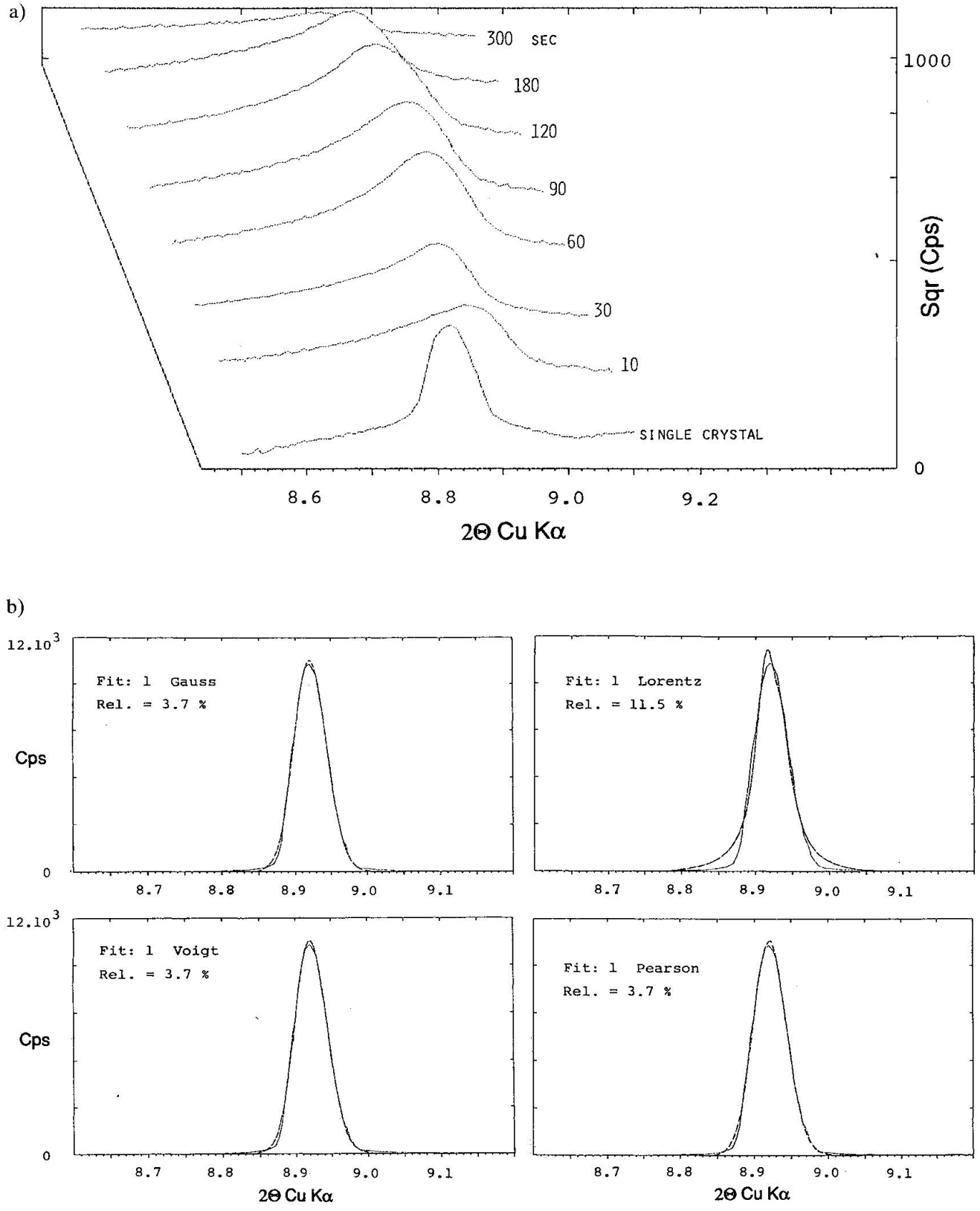

Fig. 2 Grinding experiments on muscovite and curve fitting. a) If well-crystallized single crystals of muscovite are ground with a tungsten carbide disc mill, the shape of a basal reflection changes after short grinding times, whereas the original single crystal displays a symmetric pattern. b) The latter can be fitted equally well by Gauss-, Voigt-, or Pearson functions (dashed line; measured curve = solid line), the reliability R (correspondence of measured vs calculated curve) being 3.7%. After grinding for 30 seconds (sieving fraction < 0.1 mm), the first basal reflection keeps a relatively small FWHM, but displays a strong tailing at its small Θ-angle side, resembling much a 10 Å illite complex. This tailing is, of course, not caused by the presence of two overlapping minerals (i.e. illite and a smectitic

c)

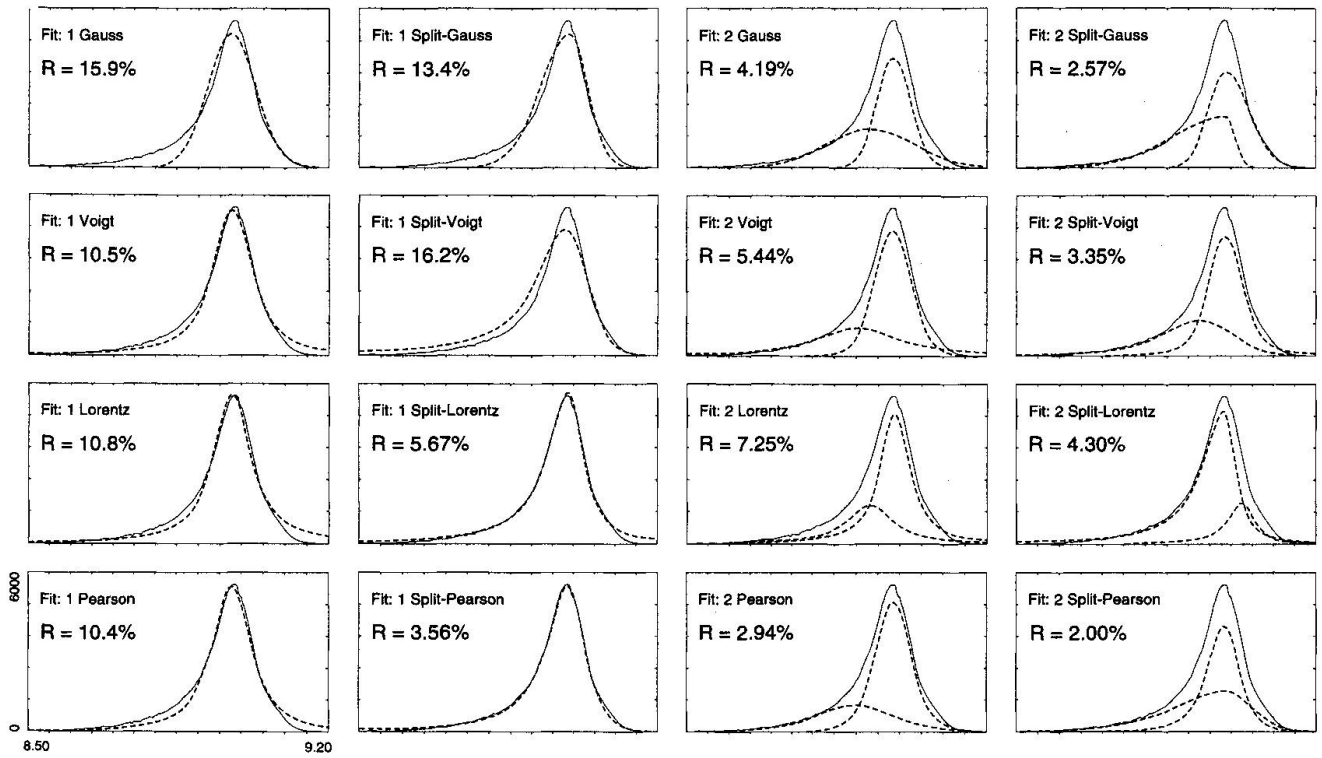

phase), but probably by the impact of grinding on the edges of mica flakes. c) Such an asymmetric reflection cannot be fitted with one single mathematical function, but with a Split-Pearson curve, STERN et al., 1993.

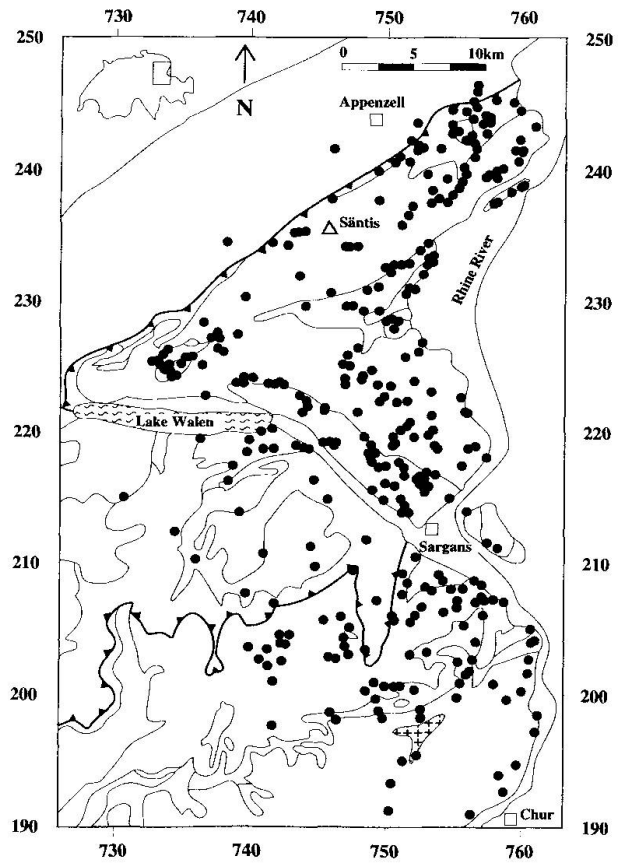

Fig. 3 Sampling localities in the study area (N = 381).

240–270 °C at a water activity of 0.6–0.8. Recently, ERDELBROCK (1994) presented a coalification map of the study area, based on about 450 vitrinite reflectance values. The thermal maturity was found to increase from ca. 0.5% Rr in the Subalpine Molasse in the north to R_{max} > 5% in the south. HUNZIKER et al. (1986) dated the main phase of Alpine metamorphism at 30–35 Ma, based on concordant K–Ar, $^{40}Ar/^{39}Ar$ and Rb–Sr illite ages, while a second age group between 20 and 25 Ma was attributed to movements along the Glarus thrust.

Results

The shape of the 10 Å complex of the investigated diagenetic and anchimetamorphic samples is dominated by the presence of a second phase besides illite-muscovite, but possibly also defined by effects of sample preparation and the brittleness of the rock samples from which clay mineral fraction are extracted. Whether a disc mill is used, or a pistill device, the mechanical impact of grinding influences the shape of a basal reflection after short grinding times already, figure 2a. A large reflection of a well crystallized mineral, like a single crystal of muscovite, may be fitted by Gauss, Voigt or Pearson functions – the meas-

Tab. 1 Instrumental conditions a): Diffractometer Siemens D-500; b): Diffractometer Philips PW-1361.

a)			
Radiation	Cu 40 kV, 30 mA. No primary filter		
Apertures	automatic entrance slit set at 3°. Secondary side 1, 0.05 and 0.15°. Graphite monochromator		
Goniometer	low angle	medium angle	high angle
	2 to 14	14 to 42	42 to 48 °2Θ
	0.05	0.02	0.02 °2Θ increment
	30	1	8 seconds per incr.
	0.10	1.2	0.15 °2Θ per minute
Computer	Sicomp 32.20 80-386 with internal and external hard discs and CD-rom for JCPDS-data sets 1-42		
Software	Diffrac AT version 3.2 by Socabim/Siemens 1993		
b)			
Radiation	Cu, 40 kV, 25 mA. Ni primary filter, no monochromator		
Slits	fixed, 2° primary side; 0.2° and 0.1 mm secondary s.		
Goniometer	angular speed 2 °2Θ per minute. Evaluation off-line from strip chart (no computer-based evaluation), curved background assumed for half-width determination		

ured and mathematically fitted curves are in any case very similar, the reliability mark is therefore nearly identical (3.7%), figure 2b. If, however, this muscovite single crystal is ground for ten seconds or longer in a disc or pistill mill, the basal reflections become asymmetric, displaying a tailing on the long-wavelength side, though the FWHM remains small. Fitting with one symmetric mathematical function yields poor reliability marks of over 10% (Fig. 2c, first column). When asymmetrical split-functions are chosen, a reliability of 3.6% is achieved by using a Pearson function, figure 2c, second column. If the measured curve is considered to consist of two symmetrical or asymmetrical overlapping curves – which is in this case of a monomineralic muscovite powder not reasonable –, good reliabilities result by the deconvolution process involved here, figure 2c, columns 3 and 4. Comparing the quality marks for the four mathematical functions used in this example (Gauss, Voigt, Lorentz and Pearson), it is evident that Pearson functions with their ability to model Gauss- and Cauchy-like shapes display the best reliabilities, and Gauss functions the worst, figure 2c, lowest row. It is obvious that FWHM do vary considerably as a function of fitting and/or deconvolution processes executed for one and the same diffractogram. Hence, the differences between data on illite reference materials (WARR and RICE, 1994) obtained by different laboratories is understandable and explained by the use of different (but not always documented) preparation and evaluation techniques. When illite crystallinity/half-width data are published, not only details on techniques of measurement, but also on sample dressing and data evaluation should therefore be presented.

The tailing of basal reflections of ground muscovite cannot be explained by the presence of a second phase like in case of the diagenetic illite complex. A possible reason for this tailing is the mechanical impact of grinding on the edges of sheet silicates, opening up the edges and widening the d-value in the crystallographic c-direction. This impact may be present also when grinding shales and slates for preparation of the < 2 micron clay fractions, as is documented by glycolated diagenetic or epizonal specimens, where no second smectitic phase has to be assumed, but an asymmetry of the first illite basal reflection is nevertheless visible, though FWHM values are small.

Incipient metamorphism of the Helvetic sediments between Säntis in the north and Chur in the south is documented by several X-ray diffraction data of clay minerals, namely:

1. The change in half-width at half peak maximum (FWHM) of the unresolved 10 Å complex (Kübler- or Scherrer-width) determined either graphically off-line, or mathematically by means of single-peak fitting (Fig. 5) shows, that for epizonal and anchimetamorphic specimens the FWHM (air-dried) of Siemens D-500 and Philips diffractograms are highly correlated ($r = 0.920$, $N = 93$, $HW < 0.5$). Since the slope of the regression line is near 1, and the intercept near zero, the literature data for HW-limits of the anchizone

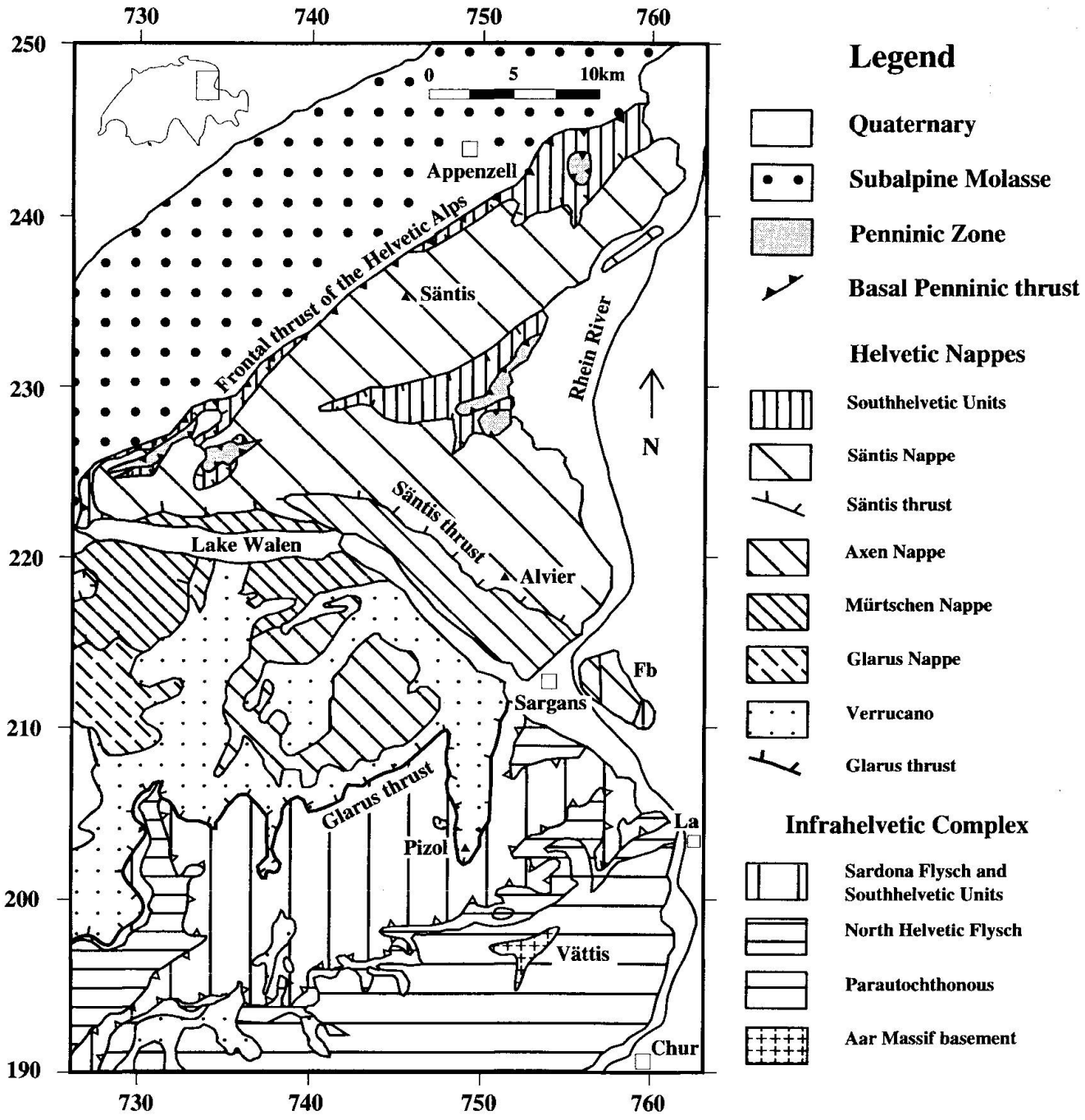

Fig. 4 Tectonic map of the study area of NE Switzerland, simplified from "Tektonische Karte der Schweiz 1 : 500 000, Schweiz. Geol. Kommission, 1980".

(0.42 and 0.25, Philips) remain valid also for diffractograms obtained by a Siemens D-500, provided that appropriate hardware conditions are chosen (Tab. 1a). For diagenetic specimens the correlation between Philips- and Siemens data seems to deviate from linearity in case of large half-widths. This may be due to the different background at low Θ-angles measured with fixed (Philip PW-1361) vs variable (Siemens D-500) entrance slits.

2. The change in half-width of the mathematically deconvoluted first basal reflection of illite is presented in figure 6 a, b. These half-widths are numerically smaller than the ones of the unresolved complex and display a close correlation for high-anchimetamorphic and epizonal specimens ($r = 0.936$, $N = 140$). But there is no correlation for diagenetic ones because of the preponderance of the smectitic phase defining the overall-HW of the unresolved complex, figure 6a. The

hatched area displays projection points of specimens containing this second, smectitic phase besides illite. Inasmuch as the peak area of the deconvoluted smectitic phase is correlated with its mass, it follows that this phase is dominant in the north of the study area, and in the upper parts of the Axen nappe, figure 7.

3. The change in half-width of the deconvoluted smectitic phase is documented in figure 8. The half-widths are numerically larger than the ones of illite and contribute predominantly to the asymmetric shape of the unresolved complex in diagenetic and anchimetamorphic air-dried specimens. Specimens with particularly low amounts of smectitic phase display a low FWHM

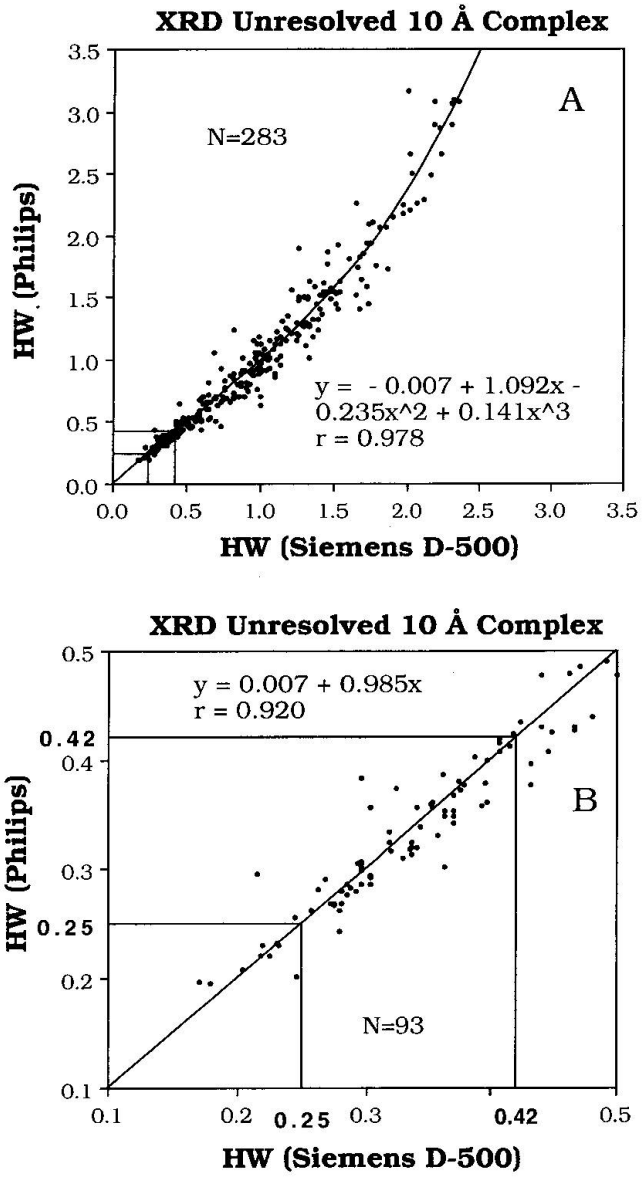

Fig. 5 Half-width of the air-dried, unresolved complex: correlation of data obtained with a Siemens D-500 and a Philips PW-1361 diffractometer. A) The regression function is linear only for the relatively small half-widths of epizonal, anchimetamorphic and highly diagenetic < 2 micron fractions. B) The boundaries of the anchimetamorphic realm – as described in literature for Philips diffractometers of the 1960/70ies – (0.25 and 0.42 °2Θ) are valid for a D-500 as well, provided that appropriate slit configurations are chosen (Tab. 1).

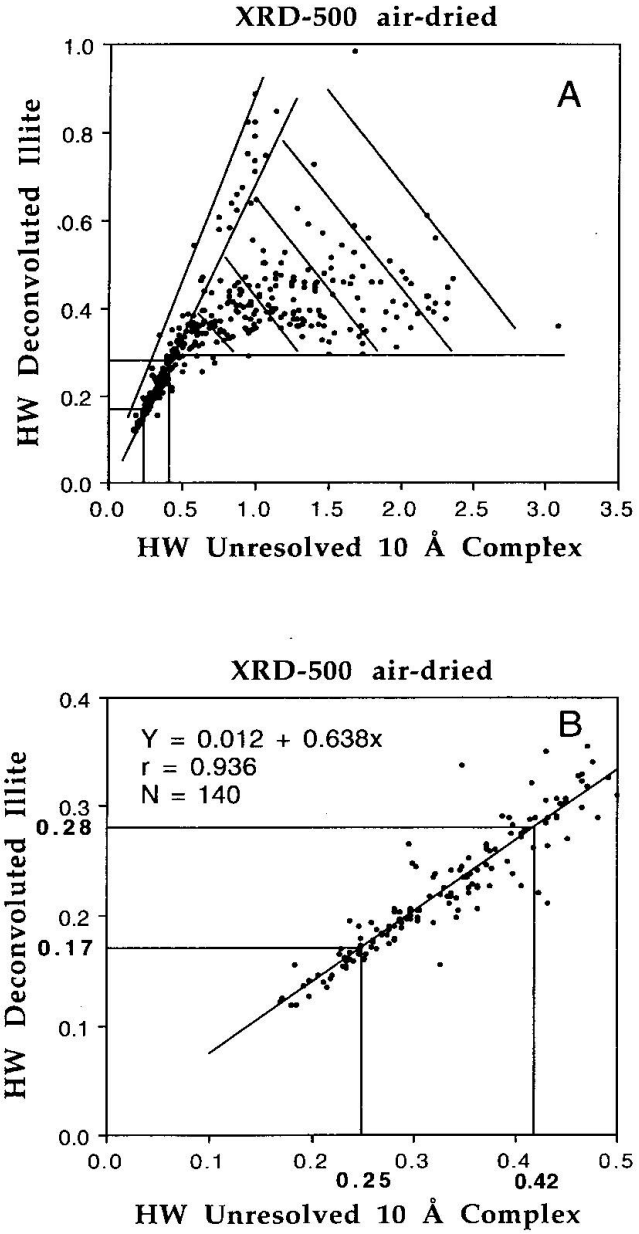

Fig. 6 Half-width of the air-dried, unresolved complex vs deconvoluted illite. A) When all diagenetic < 2 micron fractions are included, no correlation exists, since the half-width of the unresolved complex of most diagenetic specimens is dominated by its smectite content (hatched area). B) If, however, only epizonal, anchimetamorphic and highly diagenetic specimens are considered, a good correlation results with r = 0.936 for N = 140. Since the half-width of deconvoluted illite is smaller than the one of the complex, the slope of the correlation line equals 0.64.

of the unresolved complex, but high half-widths of the deconvoluted smectitic phase (circled area, see also Fig. 9a). A small part of the asymmetry may be attributed to the grinding impact, see point 6.

4. The better a clay mineral is crystallized, the smaller its FWHM and the higher the curve exponents of a Pearson fit are. Well crystallized phases display therefore a Gauss-like shape with exponents over 5, poorly crystallized a Cauchy-like with low exponents and a broad base line. Accordingly, high exponents are frequently encountered in anchimetamorphic and epizonal specimens, but no statistically proven correlation exists.

5. The change in the d-value of the deconvoluted smectitic phase is large (up to 12 Å) in diagenetic samples in the north of the area studied, but small in the south (near 10 Å), figure 9a. The projection points in the circled area represent samples with a low smectite content, where the

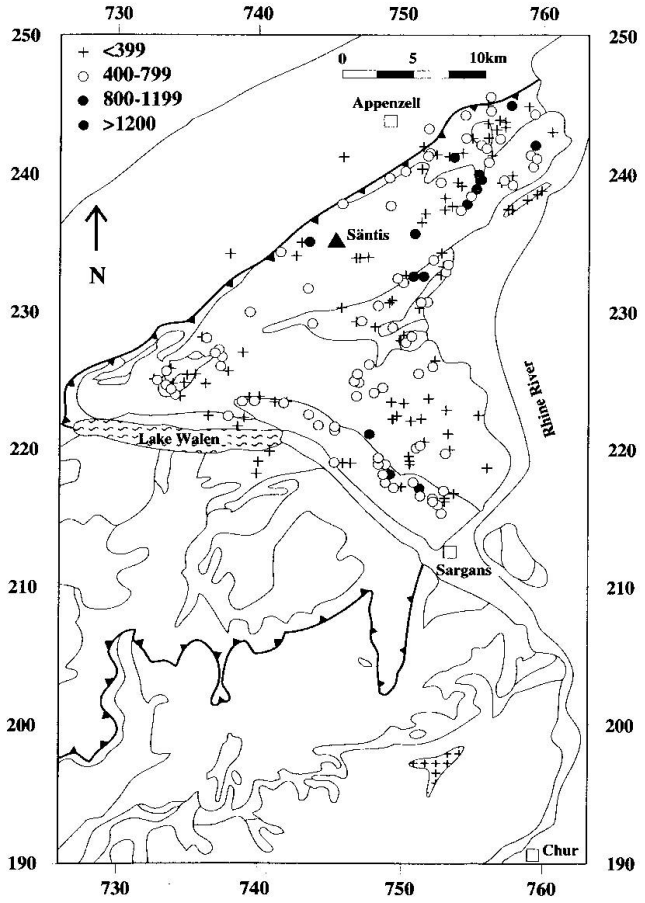

Fig. 7 Diagenetic specimens from the hatched area (Fig. 6a) plot in the northern part of the study area. The amount of smectitic phase – represented by its deconvoluted area (< 399 to < 1200) – tends to be larger in the higher elevated outcrops (e.g. Axen nappe NW of Sargans).

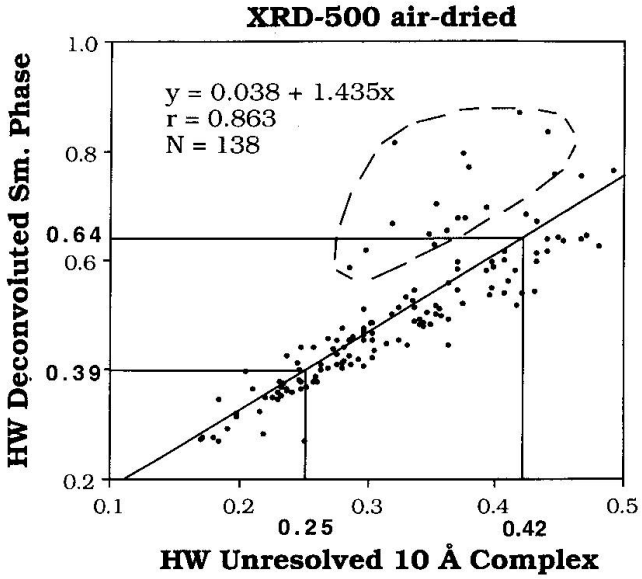

Fig. 8 Half-width of the air-dried, unresolved complex vs deconvoluted smectitic phase. Only epizonal, anchimetamorphic and highly diagenetic < 2 micron fractions are plotted, the coefficient of correlation is 0.863 with N = 138. The deconvoluted half-widths of the smectitic phase are expectedly larger than the ones of the unresolved complex, the HW-boundaries of the anchizonal air-dried specimens larger. For explanation of the circled area, see figure 10.

half-width of the 10 Å complex is defined solely by illite. If these points are disregarded, a good correlation exists between the FWHM of the unresolved complex and the d-value of the smectitic phase (r = 0.936, N = 271), figures 9b, and 9c for the epizonal/anchimetamorphic specimens (r = 0.815, N = 140). For diagenetic specimens deconvolution has a clear advantage over the unresolved complex.

6. In anchimetamorphic and epizonal specimens the FWHM of deconvoluted, air-dried and glycolated samples (unresolved complex) plot in a narrow correlation field, but are numerically different having a slope of the correlation line of 0.65, figure 10b. When the hatched, smectite-rich projection points in figure 10a are disregarded, a good correlation exists (r = 0.918, N = 135). Hence, roughly two thirds of the FWHM (unresolved complex) equal the deconvoluted FWHM of illite, one third is attributed to a tailing induced by grinding (see also point 4). When the FWHM of the air-dried, deconvoluted illite is corrected for this amount and subtracted from the complex (Fig. 10c, left y-axis: calculated fraction of smectitic phase, air-dried) and plotted against the half-width difference (measured FWHM air-dried minus glycolated, x-axis = experimentally determined fraction of smectitic

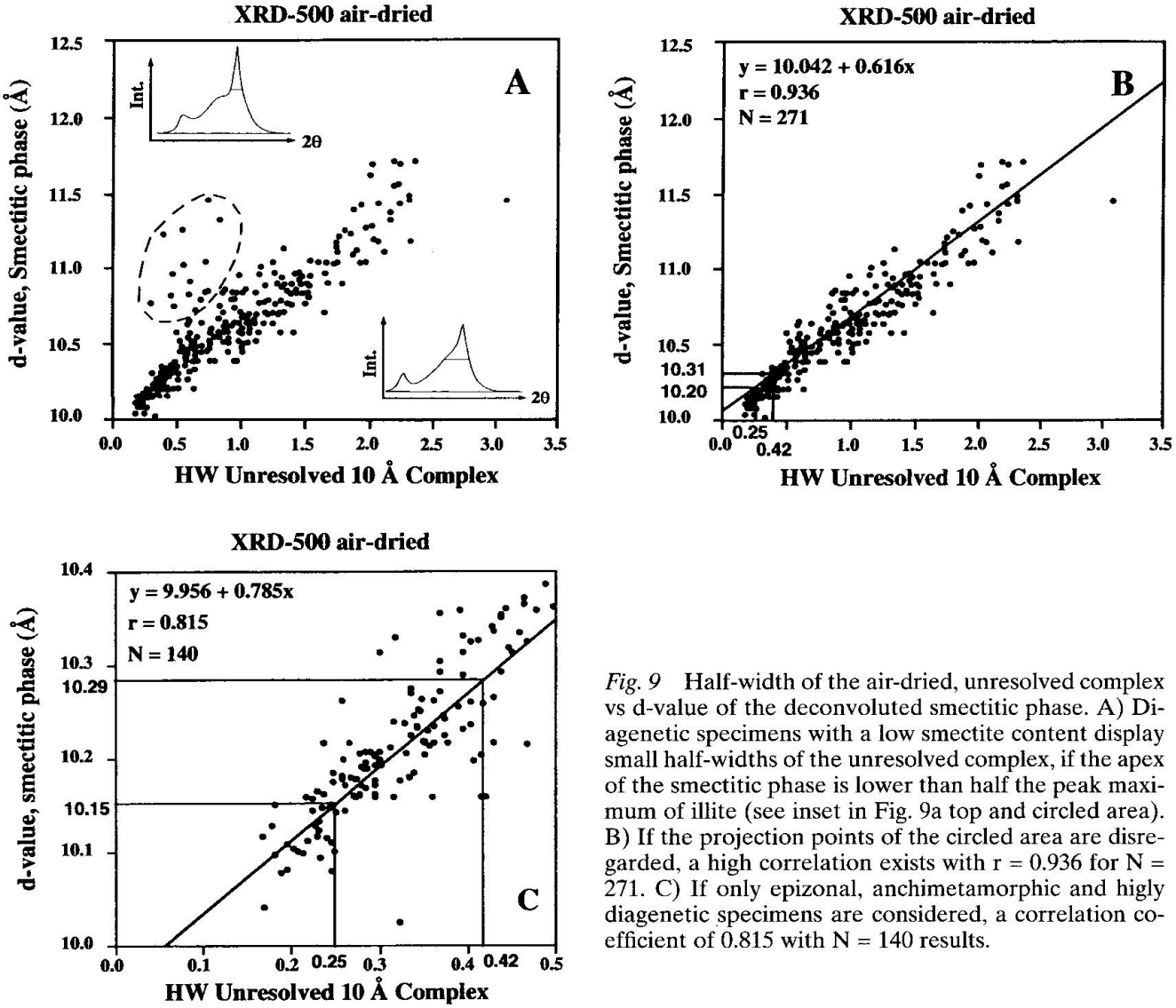

Fig. 9 Half-width of the air-dried, unresolved complex vs d-value of the deconvoluted smectitic phase. A) Diagenetic specimens with a low smectite content display small half-widths of the unresolved complex, if the apex of the smectitic phase is lower than half the peak maximum of illite (see inset in Fig. 9a top and circled area). B) If the projection points of the circled area are disregarded, a high correlation exists with r = 0.936 for N = 271. C) If only epizonal, anchimetamorphic and higly diagenetic specimens are considered, a correlation coefficient of 0.815 with N = 140 results.

phase) a correlation line with a slope close to 1 results (r = 0.971, N = 366). The second y-axis bears the FWHM of the air-dried, unresolved complex with its 0.25 and 0.42 marks for epizonal/anchimetamorphic/diagenetic boundaries. The crosspoints of the dashed lines define the average onset (0.3 to 0.6 Δ°2Θ air-dried complex) of the smectitic phase being present, and the remaining tailing due to preparational impacts respectively. As a consequence, the FWHM data of the air-dried specimens (complex and tailing-corrected, deconvoluted illite) can be used for a FWHM determination of the second, smectitic phase. The latter begins to develop in the anchimetamorphic realm (0.3 Δ°2Θ) and is predominant in the diagenetic samples.

7. Both, the half-width of the unresolved complex (Kübler index) and the data of the deconvoluted phases may be used for crystallinity studies, figure 11. The deconvoluted data display a large variability, suitable for a differentiation of the metamorphic phenomena. The crystallinity, derived from deconvoluted data, does not vary only from north to south, but also within tectonic units (e.g. Axen nappe). A particularly large variation is observed in diagenetic and anchimetamorphic d-values and FWHM of the smectitic phase.

Conclusions

Basal reflections of single crystals – e.g. muscovite – are approximately symmetrical with equal left and right widths and curve exponents. Ground single crystals, however, epizonal air-dried illite, and glycolated clay minerals display a certain asymmetry or tailing (left half-width larger than the right one), which represents roughly

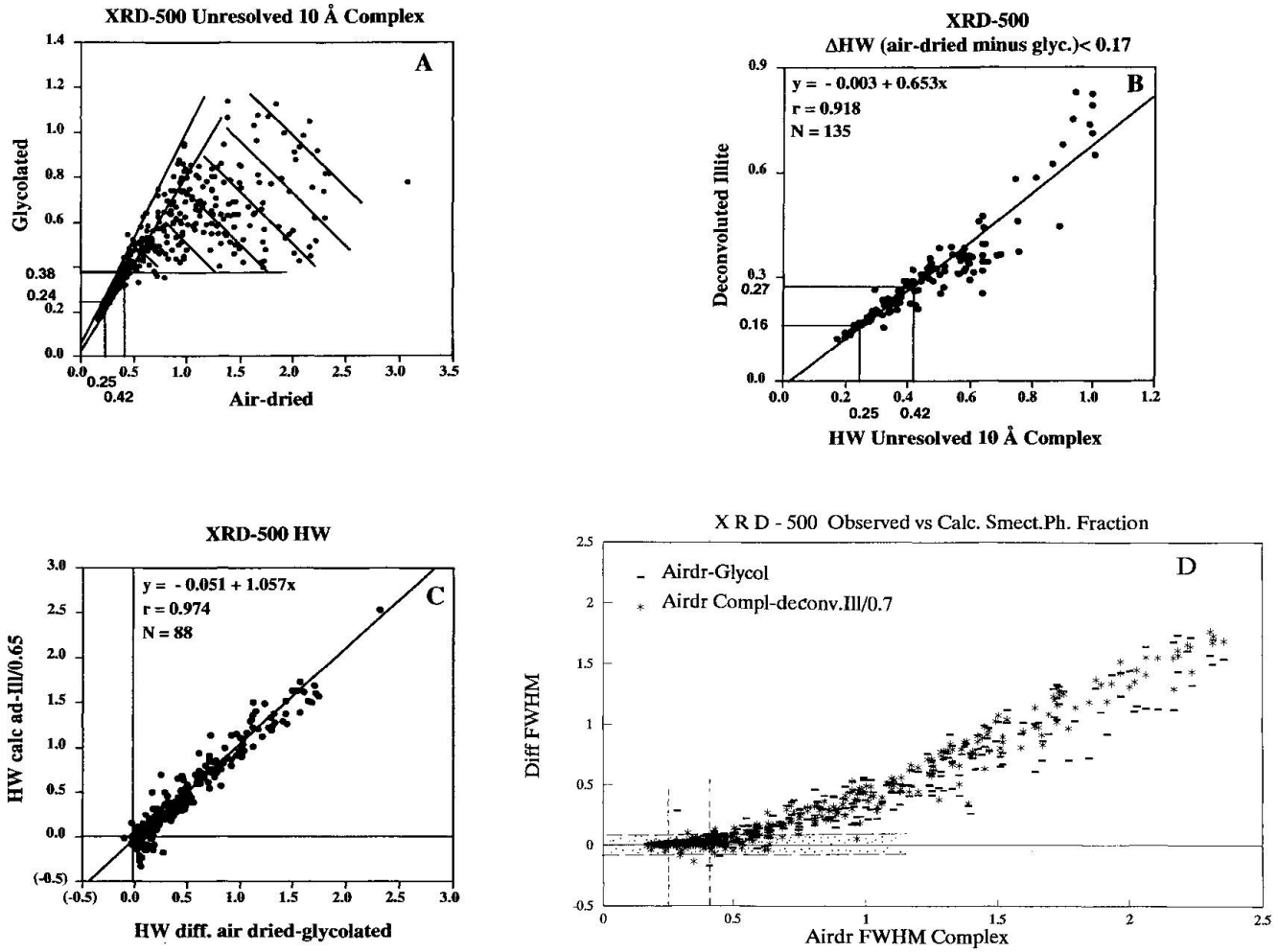

Fig. 10 Half-width of the unresolved complex: air-dried vs glycolated.
A) Most of the diagenetic specimens (hatched area) display a considerably smaller half-width after glycolation.
B) For some cases, however, the same slope of the regression line is valid as for epizonal and anchimetamorphic specimens (Fig. 10 b). Since for e.g. epizonal < 2 micron fractions the slope of the regression line equals 0.65 but not 1, one has to conclude that the unresolved air-dried complex either still contains an additional phase broadening the reflection, or displays a (small) asymmetry, which contributes to approximately one third of the entire reflection.
C) The presence of a second, smectitic phase can either be documented by the FWHM-difference of the air-dried minus glycolated complex (x-axis), or by the FWHM-difference of the air-dried complex minus deconvoluted air-dried illite, provided that the latter is corrected for its tailing induced by grinding (y-axis). The correlation is high (r = 0.974, N = 88), the slope near 1 and the intercept near zero. Hence, the second phase besides illite may be documented by comparison of air-dried and glycolated specimens, or by compairing data of air-dried specimens alone.
D) The second, smectitic phase begins on the average to disappear in the anchimetamorphic realm, where projection points (air-dried FWHM complex vs FWHM-difference) leave the dotted horizontal error zone.

one third of the total half-width. It follows, therefore, that the first clay mineral complex of air-dried < 2 micron fractions may consist of two different parts: one caused probably by sample dressing (crushing- and grinding impact on sheet silicates), and one caused by the presence of a second, smectitic phase predominant in specimens, where the FWHM of the air-dried, unresolved complex exceeds 0.3 under given preparational conditions. The smectitic phase can be evaluated either on air-dried specimens by mathematical deconvolution procedures and separation from illite, or by subtracting glycolated FWHM from the corresponding air-dried ones. The smectitic phase is dominant in diagenetic specimens and is sensitive to incipient metamorphism: with growing crystallinity its d-value, half-width and peak area becomes smaller and vanishes under anchimetamorphic conditions. The variability of these deconvoluted quantities is

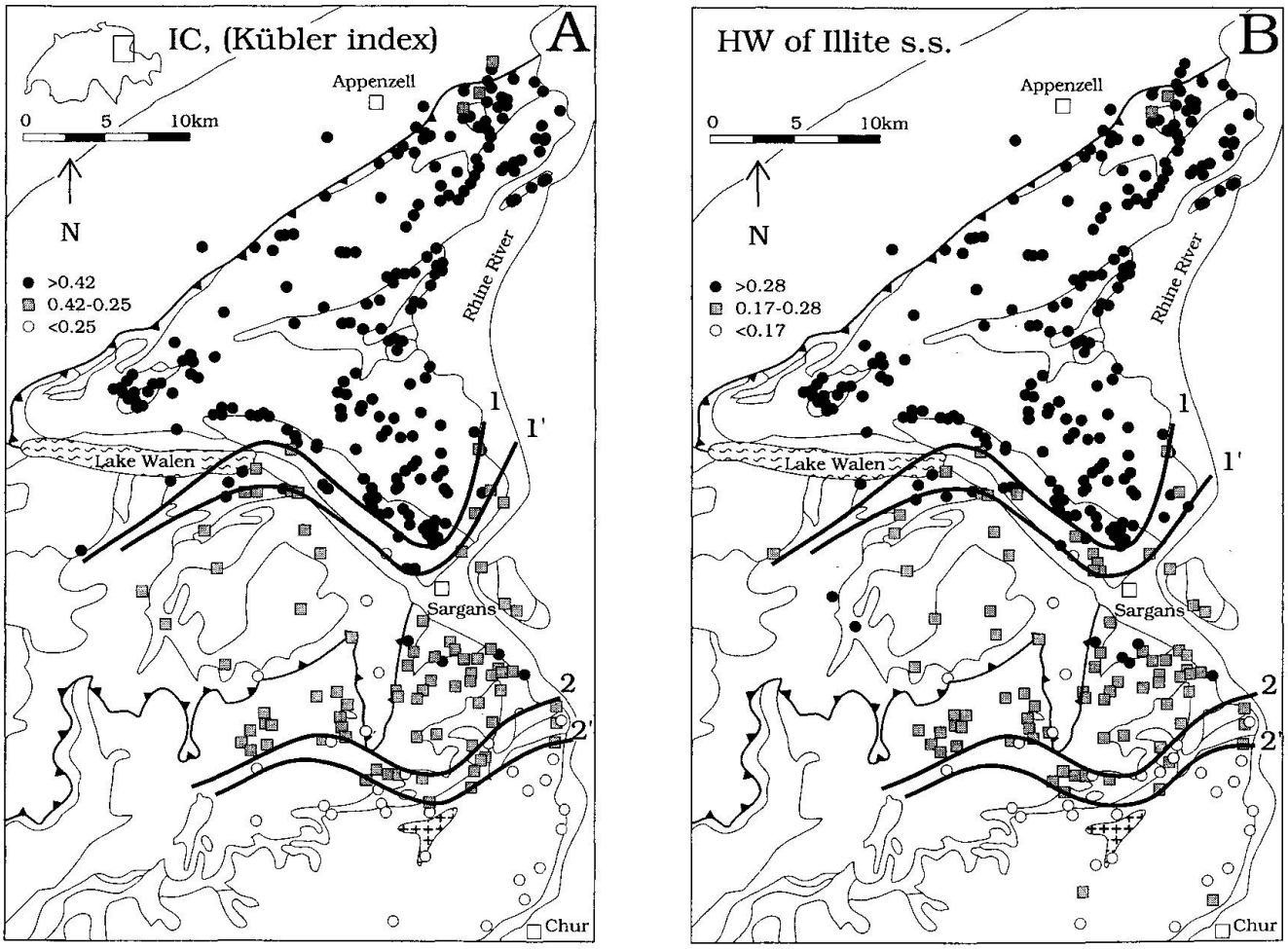

Fig. 11 "Illite" crystallinity data of the study area. The half-widths of the unresolved complex (Kübler index) are plotted in figure 11A, whereas deconvoluted HW of illite, of the smectitic phase and its d-value are plotted in figure 11B.
The deconvoluted data ex air-dried < 2 micron fractions display a quite differentiated pattern connected not only with incipient metamorphism, but also with tectonic setting and elevation above sea level.

Tab. 2 FWHM Δ°2Θ for metamorphic boundaries

unresolved 10 Å complex Kübler/Scherrer index		Pearson deconvoluted illite/smectite phase		
(1)	(2)	(3)	(4)	(5)
epizonal				
0.25	0.25	0.17	0.39	10.15
anchimetamorph				
0.42	0.42	0.28	0.64	10.29
diagenetic				

(1) Philips PW-1361 (Fig. 5)
(2) Siemens D-500 (Fig. 5)
(3) Siemens D-500 deconvoluted illite (Fig. 6)
(4) Siemens D-500 deconvoluted smectite phase (Fig. 8)
(5) d-value Å smectite phase (Fig. 9)

considerably larger than the one of illite-muscovite, they lend themselves therefore to be used as quantifiers of crystallinity/incipient metamorphism. The FWHM (Δ°2Θ) for metamorphic boundaries determined on < 2 μm fractions are shown in table 2.

In all cases where a second phase besides illite exists, simple curve fitting with symmetrical or split-functions does not match reality – deconvolution has to be performed by using either symmetrical or split-functions. Since the shape of sheet silicate basal reflections change with incipient metamorphism, any mathematical fitting should be performed with functions being able to model Gauss-like reflections (well crystallized phases) and Cauchy-like also (poorly crystallized illite), like Pearson functions.

Future work will have to correlate the refined quantities (halfwidths, d-values, peak areas of il-

lite and the smectitic phase) with fluid inclusion and coal rank data, but also with bulk rock chemistry and mineral mode, and with detailed studies of geology and tectonic setting.

Acknowledgements

The authors are indebted to dres D. Eberl (U.S. Geol. Survey, Boulder), R. Nüesch (ETH, Zürich), J. Walker (Vassar College, N.Y.) and an anonymous reviewer for critical reading and helpful suggestions.

References

DELHEZ, R., DE KEIJSER, TH.H. and MITTEMEIJER, E.J. (1982): Determination of crystallite and lattice distortions through X-ray diffraction line profile analysis, recipes, methods and comments. Fresenius Z. Anal. Chem. 312, 1–16.

ERDELBROCK, K. (1994): Diagenese und schwache Metamorphose im Helvetikum der Ostschweiz (Inkohlung und Illit-"Kristallinität"). Unpubl. Diss. Techn. Hochschule Aachen, 220 pp.

FREY, M. (1970): The step from diagenesis to metamorphism in pelitic rocks during Alpine orogenesis. Sedimentology 15, 261–279.

FREY M. (1987a): Very low-grade metamorphism of clastic sedimentary rocks. In: FREY, M. (ed.): Low Temperature Metamorphism. Blackie, Glasgow, 9–58.

FREY, M. (1987b): The reaction-isograd kaolinite + quartz = pyrophyllite + H_2O, Helvetic Alps, Switzerland. Schweiz. Mineral. Petrogr. Mitt. 67, 1–11.

FREY, M. (1988): Discontinuous inverse metamorphic zonation, Glarus Alps, Switzerland: evidence from illite "crystallinity" data. Schweiz. Mineral. Petrogr. Mitt. 68, 171–183.

FREY, M., HUNZIKER, J.C., ROGGWILLER P. and SCHINDLER, C. (1973): Progressive niedriggradige Metamorphose glaukonitführender Horizonte in den helvetischen Alpen der Ostschweiz. Contrib. Mineral. Petrol. 39, 185–218.

HUNZIKER, J.C., FREY, M., CLAUER, N., DALLMEYER, R.D., FRIEDRICHSEN, H., FLEHMIG, W., HOCHSTRASSER, K., ROGGWILLER, P. and SCHWANDER, H. (1986): The evolution of illite to muscovite: mineralogical and isotopic data from the Glarus Alps, Switzerland. Contrib. Mineral. Petrol. 92, 157–180.

KLUG, H.P. and ALEXANDER, L.E. (1974): X-ray Diffraction Procedures, John Wiley & Sons, New York.

KÜBLER, B. (1968): Evaluation quantitative du métamorphisme par la cristallinité de l'illite. Bull. Cent. Rech. Pau-SNPA 2, 385–397.

LANSON, B. and BESSON, G. (1992): Characterization of the end of smectite- to -illite transformation: decomposition of X-ray patterns. Clay & Clay Minerals 40, 40–52.

LANSON, B. and CHAMPION, D. (1991): The I/S-illite reaction in the late stage diagenesis. Amer. J. Sci. 291, 473–506.

LAUE, M.V. (1926): Lorentz-Faktor und Intensitätsverteilung in Debye-Scherrer-Ringen. Zeitschrift Krist. 64, 115–142.

STERN, W.B., MULLIS, J., RAHN, M. and FREY, M. (1991): Deconvolution of the first "illite" basal reflection. Schweiz. Mineral. Petrogr. Mitt. 71, 453–462.

STERN, W.B., MULLIS, J., RAHN, M., SUN, M. and FREY, M. (1993): On the shape of "illite" first basal reflection, crystallinity and incipient metamorphism (central Alps, Switzerland). IGCP Project 294 final meeting, 15–30 November 1993, Santiago de Chile.

STERN, W.B., MULLIS J., RAHN, M., SUN, M. and FREY, M. (1995): On the shape of the first "illite" XRD reflection, crystallinity, and incipient metamorphism. Revista Geol. Chile 21.

TRÜMPY, R. (1980): Geology of Switzerland, Part A, Wepf & Co. Publishers, Basel, New York.

VELDE, B. and LANSON, B. (1993): Comparison of I/S transformation and maturity of organic matter at elevated temperatures. Clays & Clay Minerals 41, 178–183.

WANG, H. (1994): Step size, scanning speed and shape of X-ray diffraction peak. J. Appl. Cryst. 27, 716–721.

WARR, L.N. and RICE, A.H.N. (1994): Interlaboratory standardization and calibration of clay mineral crystallinity and crystallite size data. J. metamorphic Geol. 12, 141–152.

Manuscript received December 12, 1994, revision accepted May 22, 1995.